Supporting Information

Please note: this updated document was made available on 18th June 2024, to correct an error in Fig. 6b.

Preventing lead leakage in perovskite solar cells and modules with a low-cost and stable chemisorption coating

Zongxu Zhang[a,b], Yating Shi[a,b], Jiujiang Chen [c], Peng Shen[d], Hongshi Li[d], Mengjin Yang [c], Shirong Wang[a,b], Xianggao Li[a,b], Fei Zhang[a,b*]

[a] School of Chemical Engineering and Technology, Tianjin University, Tianjin 300072, China. Email: fei_zhang@tju.edu.cn

[b] Collaborative Innovation Center of Chemical Science and Engineering (Tianjin), Tianjin 300072, China

[c] Zhejiang Engineering Research Center for Energy Optoelectronic Materials and Devices, Ningbo Institute of Materials Technology and Engineering, Chinese Academy of Sciences, Ningbo 315201, China

[d] Institute of New Energy Material Chemistry, School of Materials Science and Engineering, Renewable Energy Conversion and Storage Center, Nankai University, Tianjin 300350, P. R. China

Experimental Section

Materials

All solvents and chemicals were purchased from commercial suppliers and used as received without further purification. 4-tert-butyl pyridine (tBP, > 96%), lithium salt-bis(trifluoromethane)sulfonimide imide (LiTFSI), 2,2',7,7'-tetrakis-(N, N di-p-methoxyphenylamine)-9,9'-spirobifluorene (spiro-OMeTAD, 99.5%), methylammonium iodide (MAI), Bathocuproine (BCP) and fullerene (C_{60}) were purchased from Xi'an Polymer Light Technology. SnO_2 colloidal solution (15 wt% in H_2O) was purchased from Alfa Aesar. Acetonitrile (ACN, 99.8%), N, N-dimethylformamide (DMF, 99.8%), dimethyl sulfoxide (DMSO, 99.8%), isopropanol (IPA), chlorobenzene (CB, 99.9%), [2-(9H-carbazol-9-yl)ethyl]phosphonic acid (2PACz) and Lithium fluoride (LiF) were purchased from Sigma-Aldrich. Lead iodide (PbI_2，99.99%), Lead bromide ($PbBr_2$, 99.99%), Cesium iodide (CsI, 99.5%) formamidinium iodide (FAI, 99.5%), methylammonium bromide (MABr, 99.5%), fluorine-doped tin oxide (FTO) and indium-doped tin oxide (ITO) were purchased from Yingkou Advanced Election Technology Co., Ltd. Poly(vinyl alcohol) (PVA, alcoholysis:87.0~89.0 mol/mol, viscosity:4.6-5.4) and hydrogen peroxide (30 % in water) were purchased from Aladdin. Polydimethylsiloxane(PDMS, SYLGARD™ 184 Silicone Elastomer Kit) was purchased from Dow Corning. Sulfosuccinic Acid (SSA, 70 wt. % in H_2O) was purchased from Macklin.

Preparation of PDMS with SMP coating

SYLGARD™ 184 Silicone Elastomer Kit was used according to instructions and prepared into a 500 μm PDMS substrate through blade-coating. The PVA solution was prepared by dissolving 3g of PVA in 8 ml of deionized water, stirring at 90 ℃ for 30 minutes. Then，2mL of SSA was added and stirred for 30 min at 90 ℃ to obtain the blending solution. The thickness of the scraper was adjusted, and the blending solution was cast onto the PDMS substrate. PDMS with SMP coating was obtained after drying in a Vacuum oven at 45 °C for 24h.

Device Fabrication

n-i-p structure: FTO glass substrates were sequentially cleaned with deionized water, IPA, and ethanol for 15 min, respectively. Then, the glass substrates were dried by N2. The cleaned and dry FTO glass substrates were treated with ultraviolet ozone for 10 min and then transferred into an N_2-filled glovebox before use. Then, the FTO

glass substrates were spin-coated with a thin layer of SnO_2, diluted in water at a 1:5 ratio at 3,000 rpm for 30 s, followed by annealing at 150 °C for 30 min. The precursor of perovskite $(FA_{0.65}MA_{0.20}Cs_{0.15})Pb(I_{0.8}Br_{0.2})_3$ film was prepared by dissolving FAI, CsI, MABr, PbI_2, and $PbBr_2$ with stoichiometry in anhydrous N, N-dimethylformamide (DMF) and dimethyl sulfoxide (DMSO) mixed solvent (4/1, v/v). Then, 60 μL, 1.5M perovskite precursor was coated on the SnO_2/FTO substrate at a spin speed of 2,000 rpm for 10 s and 6,000 rpm for 30 s with subsequent annealing for 60 min at 100 °C. Subsequently, the spiro-OMeTAD solutions were prepared by dissolving 90.5 mg of spiro-OMeTAD in 1 mL CB, with the addition of 35.5 μL of tBP and 20.63 μL of LiTFSI (520 mg dissolved in 1 mL of ACN). The solution was spun at 3,000 rpm for 30 s. 80 nm gold was thermally deposited for the top electrode at an evaporation rate of $0.2 \sim 0.8$ Å s^{-1}.

p-i-n structure: ITO glass substrates were sequentially cleaned with deionized water, IPA, and ethanol for 15 min, respectively. Then, the glass substrates were dried by N_2. The cleaned and dry ITO glass substrates were treated with ultraviolet ozone for 10 min and then transferred into an N_2-filled glovebox before use. Then, the ITO glass substrates were spin-coated with a thin layer of 2PACz and 4MeO-PACz(3:2 v/v, 0.5mg/mL), diluted in ethanol at 3,000 rpm for 30 s in an N_2 glovebox, followed by annealing at 100 °C for 10 min. The precursor of perovskite $FA_{0.8}MA_{0.15}Cs_{0.05}PbI_3$ film was prepared by dissolving FAI, CsI, MABr, MAI, and Pbl_2 with stoichiometry in anhydrous N, N-dimethylformamide (DMF) and dimethyl sulfoxide (DMSO) mixed solvent (4/1, v/v). Then, 60 μL, 1.5M perovskite precursor was coated on the SAMs/ITO substrate at a spin speed of 1,000 rpm for 10 s and 5,000 rpm for 30 s with subsequent annealing for 45 min at 100 °C to form the perovskite film. Subsequently, 1 nm LiF, 20 nm C_{60}, 5 nm BCP, and 100 nm silver were sequentially evaporated to complete the single-junction devices.

Module fabrication

FTO glass substrates (5 cm × 5 cm) were scribed P1 lines with a femtosecond 1030nm laser scriber, Then FTO was washed with detergent, deionized water, acetone, and isopropanol in sequence for 30 minutes. After that, the cleaned FTO substrate was dried with N_2 gas and then treated with plasma for 5 minutes. The 500μL MeO-2PACz (0.5mg/mL) dissolved in absolute ethanol as a hole transport material was spin-coated on FTO for the 30s at 3000 rpm and then annealed at 100°C for 10 minutes.

Subsequently, 350μL 1.5 M perovskite precursor was deposited on the MeO-2PACz layer. The dispersed perovskite solution was spin-coated with 4000 rpm for 25 s. Nitrogen flow was employed with the assistance of nucleation. After that, the perovskite film was quickly transferred to a hot plate at 100 °C for 30 min annealing. Then, 25 nm C60 at a rate of 0.2 Å s^{-1} and 6 nm BCP at a rate of 0.2 Å s^{-1} were thermally evaporated, respectively, under high vacuum (< 8×10^{-4} Pa). P2 was processed parallel to P1 lines using the same laser scriber to expose bottom FTOs. After that, a 100 nm silver electrode at a rate of 2.0 Å s^{-1} was thermally evaporated under a high vacuum (< 8×10^{-4} Pa). Finally, P3 lines were scribed to separate sub-cells. The distance between P1 and P3 was ~224um, the width of the subcell was 6.4mm, the aperture area of the minimodule was 10.24cm^2, and GFF was 96.5%.

Device encapsulation

Copper wires are bonded to the electrode through a conductive silver paste to lead out the electrode. Then, tightly adhere the encapsulation layer to both sides of the device and use Kraft K-704B as the edge sealant to encapsulate the device. Subsequently, place the device at room temperature for curing.

Characterization

The concentration of the Pb^{2+} aqueous solution was determined using a SHIMADZU AA-7000 atomic absorption spectrophotometer instrument. The transmittance of PDMS with or without SMP was determined using a Techcomp UV2600 UV-Vis spectrophotometer. The infrared spectra were determined using an FTIR-650. Tensile measurement was determined using an MTS CMT6103 Electronic universal testing machine (Executive standards: GB 13022-1991,[1] Sample width: 20 mm). An Analytik Jena Multi C/N 3100 determined the total organic carbon analysis. The thermogravimetric analysis was determined using a HITACHI STA200. XPS spectra were performed using a ThermoFisher Scientific K-Alpha+, Al Ka as the X-ray source, and the binding energy was calibrated with polluted carbon C1s (284.80 as the correction value) under vacuum conditions of 5×10^{-8} Pa.

J-V curves

J–V measurement of the perovskite solar cells was determined using a Keithley 2400 source meter under simulated AM 1.5G illumination with an intensity of 100 mW cm^{-2} from a solar simulator in an N_2-filled glovebox at room temperature. All *J-V* results

are measured by scanning along the reverse and forward scans in the range of -0.1 V to 1.2 V with a step volt of 0.02 V and a delay time of 10 ms. The device area was defined and characterized as 0.09 cm^2 by a metal shadow mask.

The adsorption kinetics of Pb^{2+}

In the adsorption experiment, the calculation formulas for the adsorption capacity at any time (q_t, mg g^{-1}) and at equilibrium (q_e, mg g^{-1}) are as follows:

$$q_t = \frac{c_0 - c_t}{M} V$$

$$q_e = \frac{c_0 - c_e}{M} V$$

Where C_0 represents the initial concentration of the lead ion solution (mg L^{-1}), C_t is the concentration of the lead ion solution at any time (mg L^{-1}), C_e is the concentration of the lead ion solution at equilibrium(mg L^{-1}), M is the weight of the adsorbent, and V is the volume of the lead ion solution.

Adsorption kinetics data will be fitted using pseudo-first-order and pseudo-second-order kinetic models. The equations for these two kinetic models are as follows:

Pseudo-first-order kinetic model:

$$q_t = q_e \left(1 - e^{-k_1 t}\right)$$

Pseudo-second-order kinetic model:

$$q_t = \frac{k_2 q_e^2 t}{1 + k_2 q_e t}$$

Where it is the adsorption capacity at the time, q_e is the adsorption capacity at equilibrium, k_1 is the rate constant for pseudo-first-order kinetics, k_2 is the rate constant for pseudo-second-order kinetics, and t is the time.

Computational details

All calculations were performed using the Gaussian 16 package. The geometry of the investigated structures was optimized using the B3LYP basis set with basis set superposition error (BSSE)[2].

$$E_{(interaction)} = E_{(AB)} - E_{(A)} - E_{(B)} - E_{(BSSE)}$$

Where $E_{(AB)}$ is the total energy of A model with B, $E_{(A)}$ is the energy A, and $E_{(B)}$ is that for B. $E_{(BSSE)}$ is the BSSE energy.

The estimated cost for SMP coating

For 400 μm SMP coating, the estimated usage of raw materials is ~202 g m^{-2} of PVA and ~193g m^{-2} for SSA. Wholesale prices for large quantities of raw materials: PVA costs $1.5 per kilogram (https://www.100ppi.com/mprice/plist-1-1211-1.html), SSA costs $25 per kilogram (https://china.guidechem.com/cas/481405.html). Then, the cost can be calculated as approximately $5.13 m^{-2}. For a more manufacturable p-i-n module configuration, the direct manufacturing cost is $31.7 m^{-2}.[3] When SMP film is applied to this module, the manufacturing cost increases is 16% higher than that without SMP, and the minimum sustainable price is raised to approximately 0.24 $ W^{-1},(Without SMP is 0.21 $ W^{-1}) which is still lower than that of c-Si (0.25-0.27 $ W^{-1}).[4]

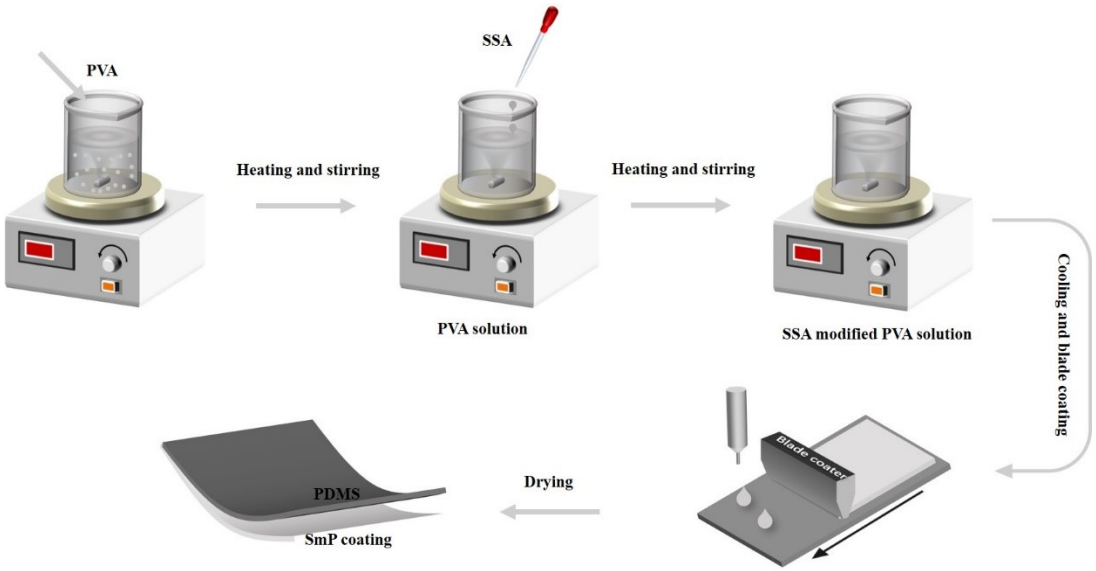

Fig. S1 Schematic diagram of SMP coating production process.

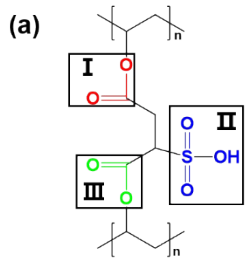

(b)

Groups	Binding Energy (kacl mol^{-1})
I	-124.30
II	-253.44
III	-220.29

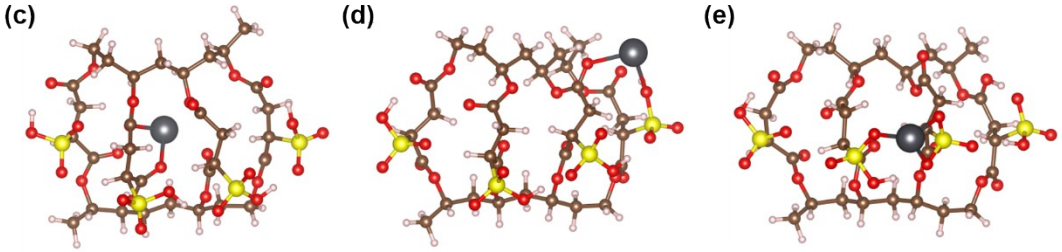

Fig. S2 (a) Structural formula of SMP. (b) Calculated binding energies (E_b) of adsorption of Pb^{2+} by different functional groups of SMP at 25 °C. Schematic of binding configurations of Pb^{2+} with different functional groups of SMP (n=4). (c) group I (d) group II (e) group III. Configurations were obtained based on density functional theory calculations.

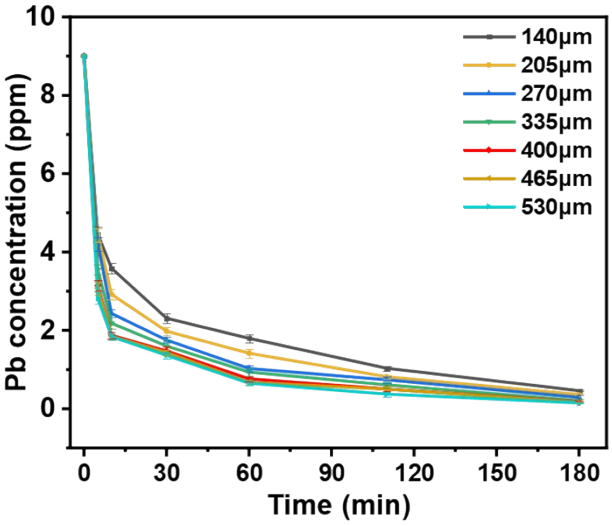

Fig. S3 The concentration changes of lead ions in the 50 mL water with an initial concentration of 9 ppm when immersing different thicknesses of 6.25 cm^2 SMP in water.

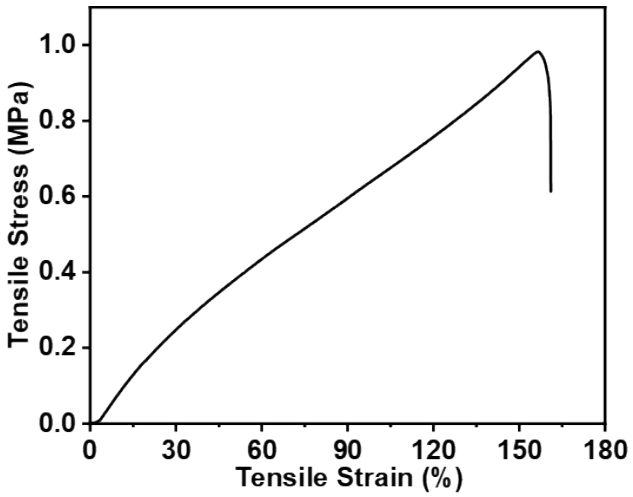

Fig. S4 Tensile curve of SMP film.

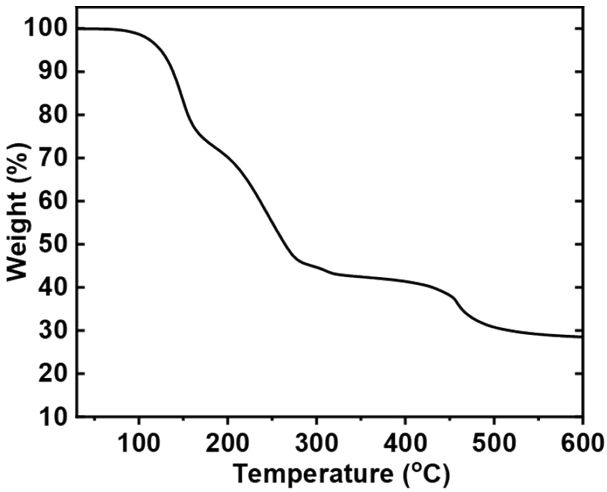

Fig. S5 TGA curves of SMP with a heating rate of 10 ^{o}C min^{-1} under nitrogen atmosphere.

(a)

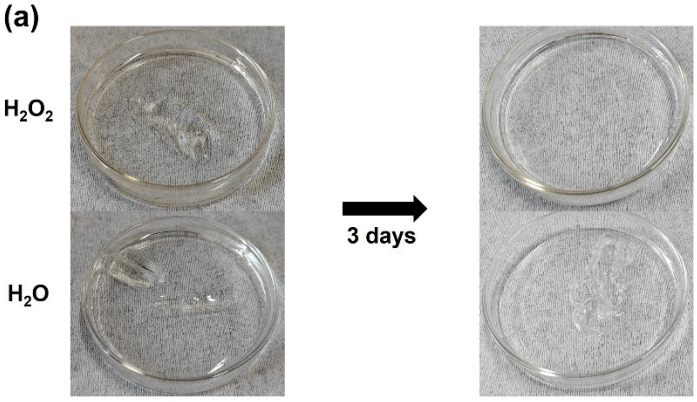

(b)

Samples	TOC (mg L^{-1})
In H_2O_2	10.23
In H_2O	0.34

Fig. S6 (a) Schematic diagram of SMP film degradation (b) the total organic carbon (TOC) results of placing 0.3g SMP in 10 mL H_2O and 10 mL H_2O_2 after 3 days.

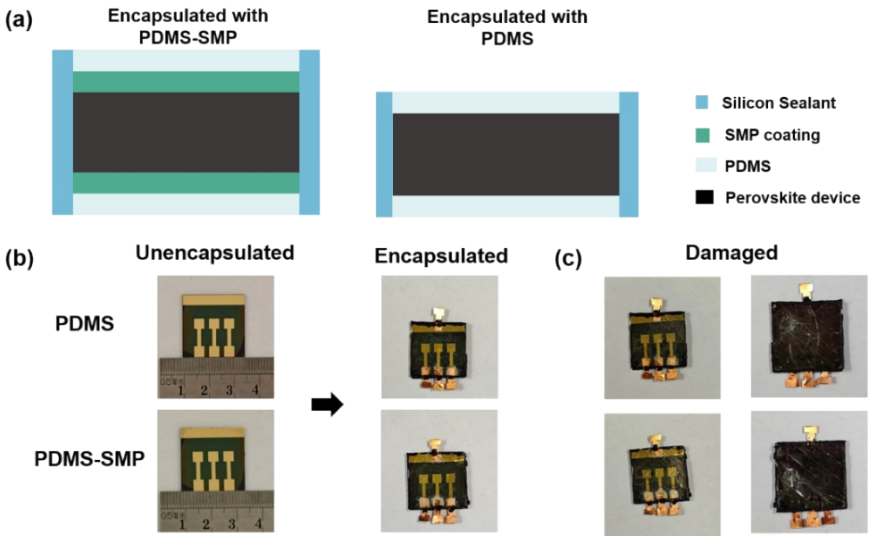

Fig. S7 (a) Two encapsulation structures with and without SMP coating. (b) Photos of two encapsulation structures in PSC devices before and after encapsulation. (c) Photos of encapsulated devices damaged with a knife and iron ball.

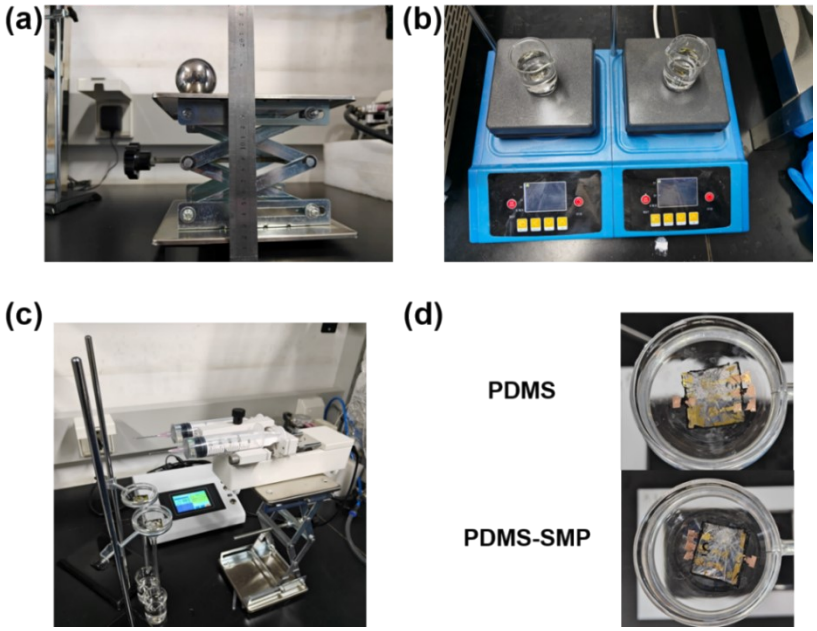

Fig. S8 Experimental setup diagram. (a) Releasing an iron ball from a vertical distance of 15 centimeters. (b) immersion test, (c) Dropping water test. (d) Photos of PSCs devices with two different encapsulation structures after rain experiment.

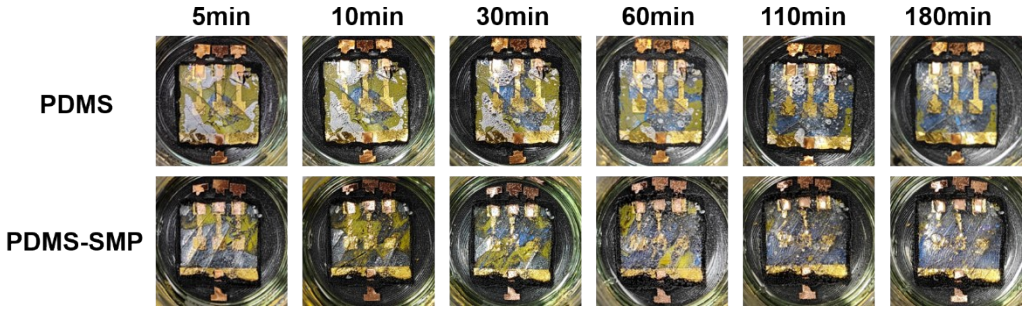

Fig. S9 Photos of the changes in n-i-p structure devices with two encapsulation structures immersed in deionized water (pH=7, 50 °C) for 180 minutes.

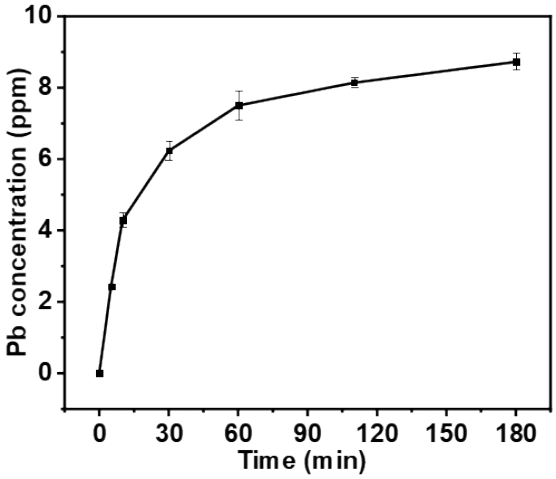

Fig. S10 The lead leakage from the bare n-i-p devices immersed in deionized water (pH=7, 25 ^{o}C) for 180 minutes.

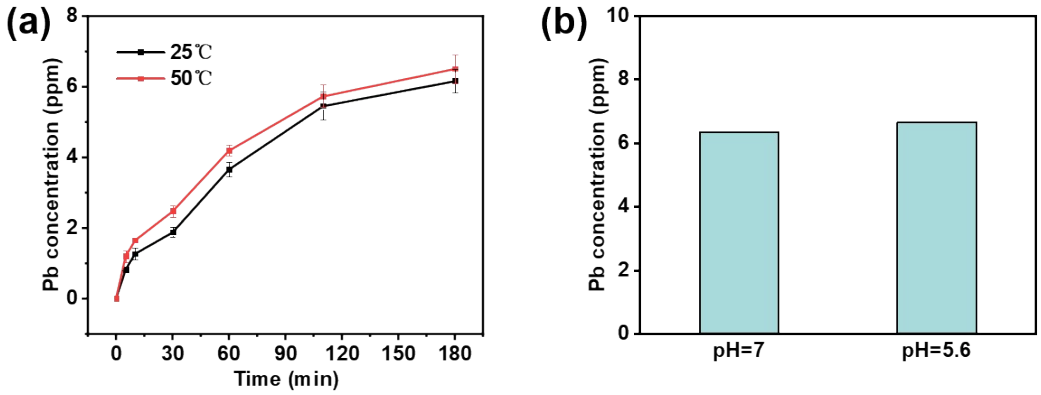

Fig. S11 Lead leakage of damaged encapsulated n-i-p devices with PDMS-PVA films. (a) Immersed in 50mL of deionized water (pH=7) for 180 minutes. (b) Simulated rainfall experiment with a flow rate of 31.25 mL h^{-1} and a duration of 1.5h.

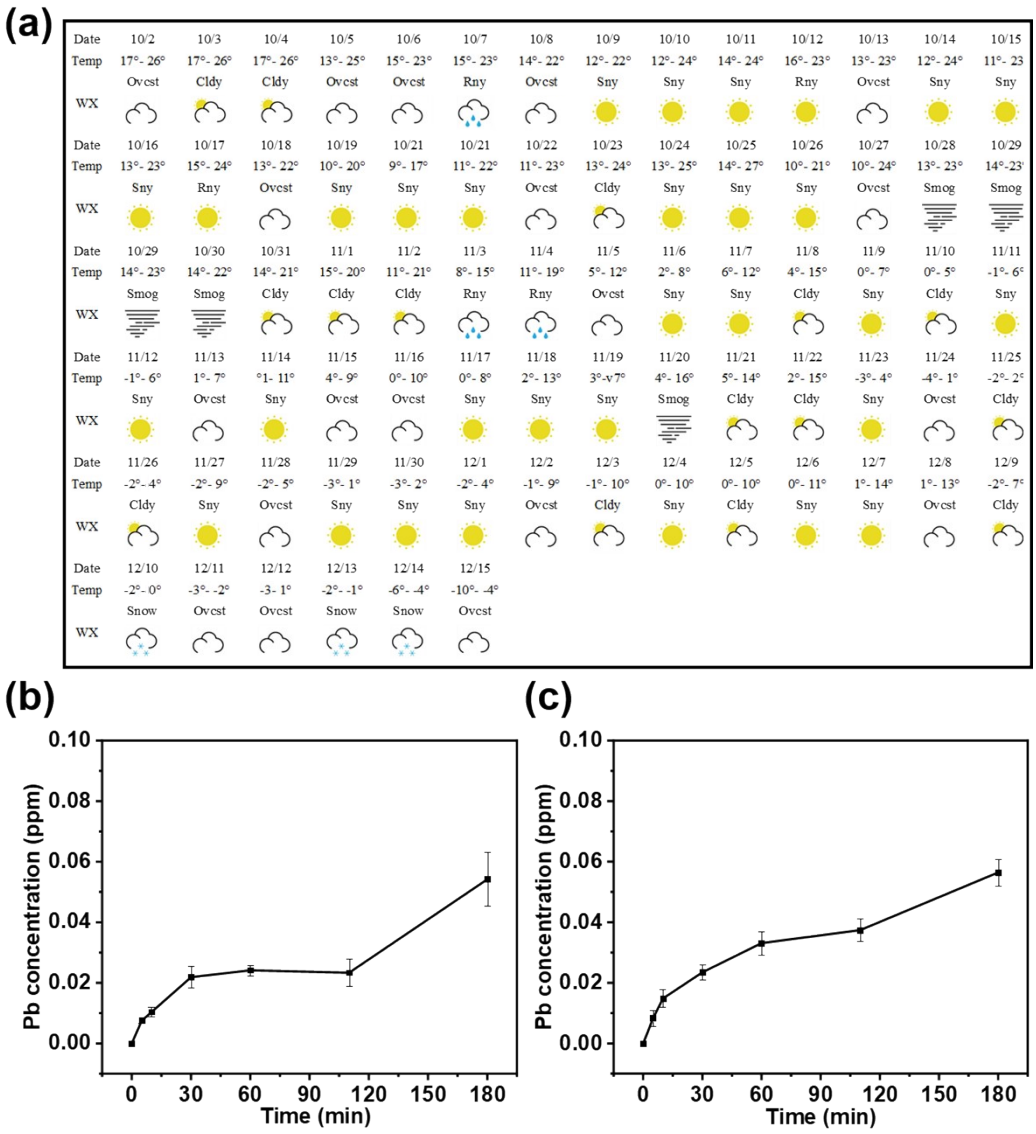

Fig. S12 (a) The specific weather conditions over the 75 days. (b) The lead leakage from the damaged devices encapsulated with the fresh PDMS-SMP film. (c) The lead leakage from the damaged devices encapsulated with the PDMS-SMP films after a 75-day outdoor exposure.

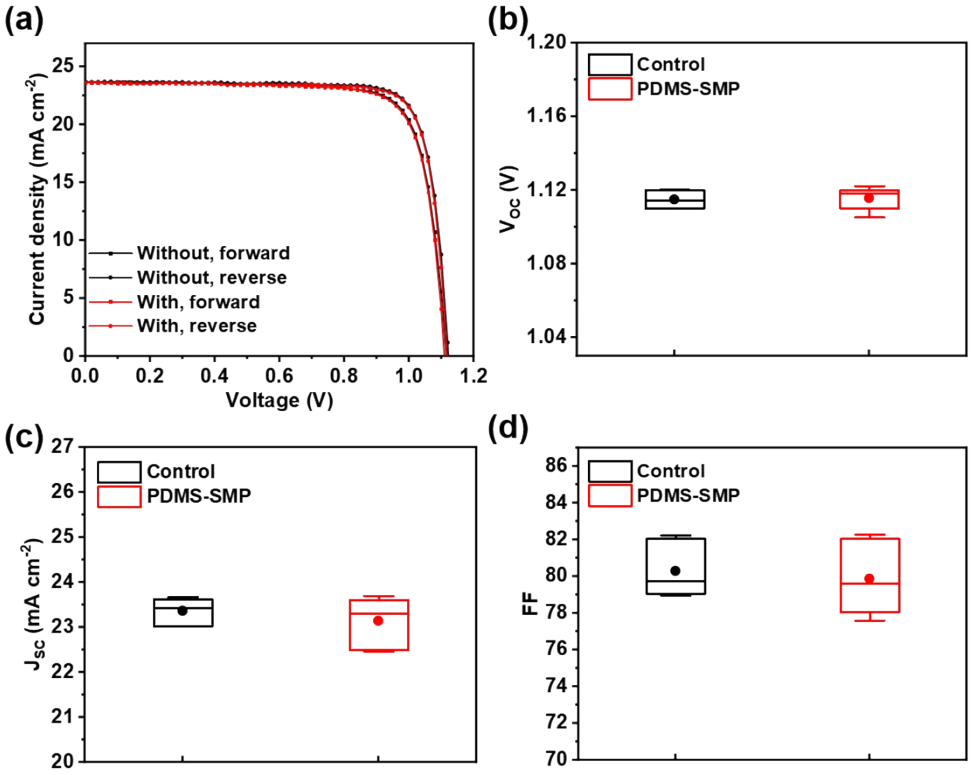

Fig. S13 (a) *J*–*V* curves of representative n-i-p PSCs devices with and without PDMS-SMP encapsulation. (b) V_{OC} (c) J_{SC} (d) FF Changes of corresponding n-i-p structure devices.6 devices in each.

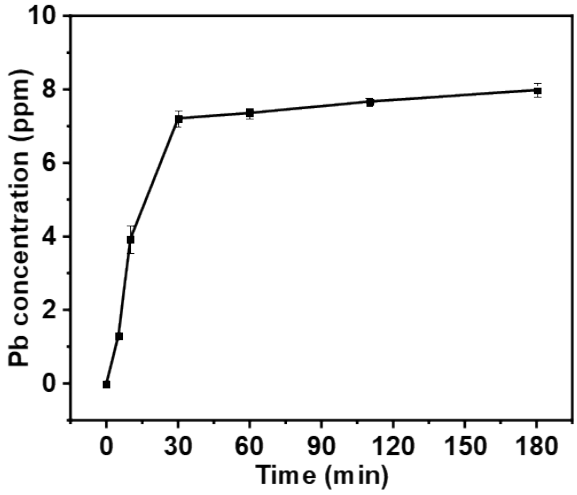

Fig. S14 The lead leakage from the bare p-i-n devices immersed in deionized water (pH=7, 25 ^{o}C) for 180 minutes.

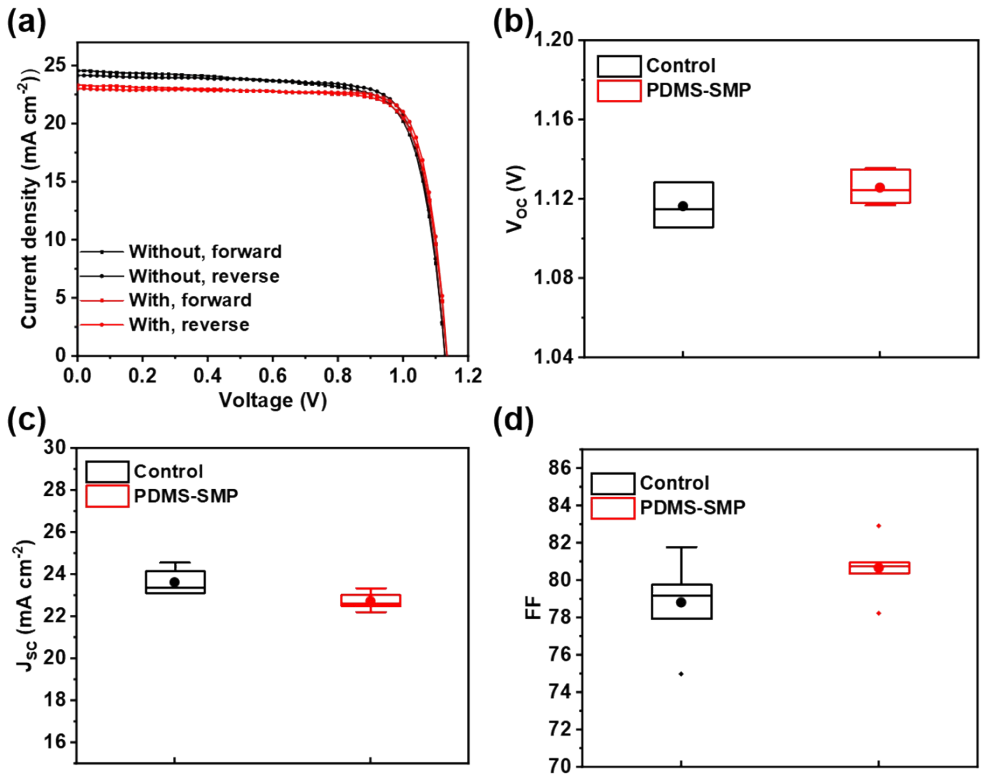

Fig. S15 (a) *J*–*V* curves of representative p-i-n PSCs devices with and without PDMS-SMP encapsulation. (b) V_{OC} (c) J_{SC} (d) FF Changes of corresponding p-i-n structure devices. 6 devices in each.

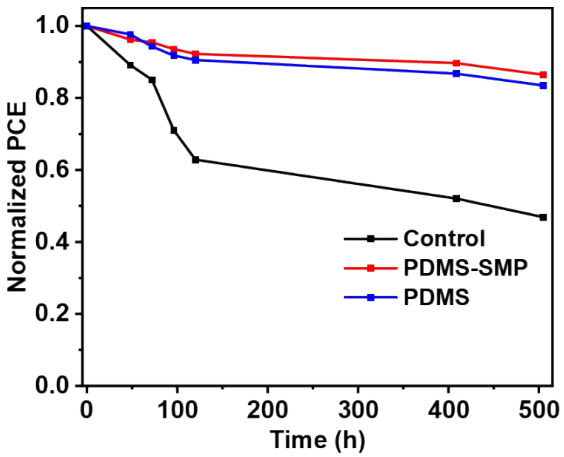

Fig. S16 The thermal stability of p-i-n PSCs encapsulated with PDMS-SMP, PDMS and control at 65 ^{o}C in an N_2-filled glovebox.

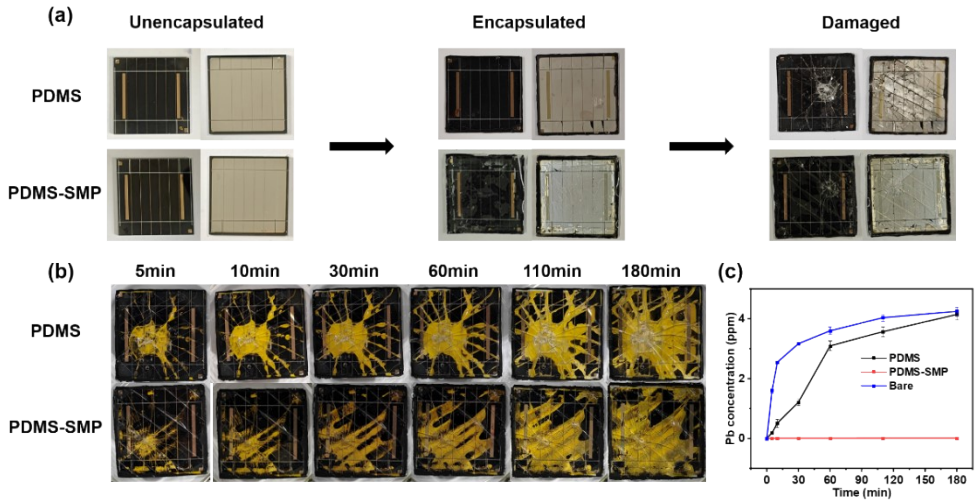

Fig. S17 (a) Photos of two encapsulation structures in p-i-n PSCs modules before and after encapsulation. (**b**) Photos of the changes in p-i-n PSC modules with two encapsulation structures immersed in deionized water (pH=7, 25 ^{o}C) for 180 minutes. The damaged PSC modules were immersed in 200ml of deionized water. (**c**) The damaged PSC modules were immersed in 200ml of deionized water (pH=7). Chart of changes in Pb^{2+} concentration in deionized water.

Table S1. Parameters for fitting adsorption kinetics models.

Kinetic Model	Parameter	
Pseudo-first-order	q_e (mg g^{-1})	1.2113
	k_1	0.2322
	R^2	0.9778
Pseudo-second-order	q_e (mg g^{-1})	1.1745
	k_1	0.3565
	R^2	0.9926

Table S2. Comparison of cost, SQE, fast-degradation between different methods.

Ref	Cost ($ M^{-2})	SQE(%)	Fast-degradation
DMDP[5]	371	96	N
EDTMP[5]	77	96	N
DMDP[6]	2470	99	N
Ionogel[7]	5.08	99	N
CFDP[8]	N	98	N
AHMA[9]	N	96	N
SmP (This work)	**5.13**	**99**	**Y**

Table S3. Photovoltaic parameters of representative n-i-p PSCs devices with and without PDMS-SMP encapsulation.

Samples	V_{OC} (V)	J_{SC} (mA cm$^{-2)}$	FF(%)	PCE (%)
Without, forward	1.12	23.65	79	20.9
Without, reverse	1.12	23.67	82	21.7
With, forward	1.11	23.60	79	20.7
With, reverse	1.12	23.60	82	21.7

Table S4. Photovoltaic parameters of representative p-i-n PSCs devices with and without PDMS-SMP encapsulation.

Samples	V_{OC} (V)	J_{SC} (mA cm$^{-2)}$	FF(%)	PCE (%)
Without, forward	1.13	24.56	75	20.8
Without, reverse	1.13	24.14	78	21.3
With, forward	1.13	23.34	78	20.6
With, reverse	1.14	23.01	81	21.2

Reference:

1. https://std.samr.gov.cn/gb/. Plastics--Determination of tensile properties of films.
2. T. Lu and Q. Chen, *Computational and Theoretical Chemistry*, 2021, **1200**, 113249.
3. Z. Song, C. L. McElvany, A. B. Phillips, I. Celik, P. W. Krantz, S. C. Watthage, G. K. Liyanage, D. Apul and M. J. Heben, *Energy & Environmental Science*, 2017, **10**, 1297-1305.
4. M. W. Brittany L. Smith, Kelsey A. W. Horowitz, Timothy J. Silverman, Jarett Zuboy, Robert M. Margolis, 2021, **NREL/TP-7A40-78173**.
5. X. Li, F. Zhang, H. He, J. J. Berry, K. Zhu and T. Xu, *Nature*, 2020, **578**, 555-558.
6. X. Li, F. Zhang, J. Wang, J. Tong, T. Xu and K. Zhu, *Nature Sustainability*, 2021, **4**, 1038-1041.
7. X. Xiao, M. Wang, S. Chen, Y. Zhang, H. Gu, Y. Deng, G. Yang, C. Fei, B. Chen, Y. Lin, M. D. Dickey and J. Huang, *Sci Adv*, 2021, **7**, eabi8249.
8. T. Wang, J. Yang, Q. Cao, X. Pu, Y. Li, H. Chen, J. Zhao, Y. Zhang, X. Chen and X. Li, *Nat Commun*, 2023, **14**, 1342.
9. Q. Wei, X. Huo, Q. Fu, T. Wang, H. Zhao, Y. Wang, J. Yang, S. Zhan, L. Zhou, S. Wang and P. Yin, *Journal of Materials Chemistry C*, 2022, **10**, 8972-8978.